Cationic Covalent Triazine Network: A Metal-Free Catalyst for Effective Acetylene Hydrochlorination

Zhaobing Shen [1,2], Ping Xing [1,3], Ke Wen [2] and Biao Jiang [1,2,3,*]

[1] Shanghai Green Chemical Engineering Research Center, Shanghai Institute of Organic Chemistry, No. 345 Lingling Road, Shanghai 200032, China

[2] Green Chemical Engineering Research Center, Shanghai Advanced Research Institute, Chinese Academy of Sciences, No. 99 Haike Road, Zhangjiang Hi-Tech Park, Pudong, Shanghai 201210, China

[3] National Laboratory for Advanced Fluorine and Nitrogen Material, Shanghai Institute of Organic Chemistry, Lingling Road 345, Shanghai 200032, China

* Correspondence: jiangb@sioc.ac.cn; Tel.: +86-021-5492-5566

Abstract: Vinyl chloride, the monomer of polyvinyl chloride, is produced primarily via acetylene hydrochlorination catalyzed by environmentally toxic carbon-supported $HgCl_2$. Recently, nitrogen-doped carbon materials have been explored as metal-free catalysts to substitute toxic $HgCl_2$. Herein, we describe the development of a cationic covalent triazine network (cCTN, cCTN-700) that selectively catalyzes acetylene hydrochlorination. cCTN-700 exhibited excellent catalytic activity with initial acetylene conversion, reaching ~99% and a vinyl chloride selectivity of >98% at 200 °C during a 45 h test. X-ray photoelectron spectroscopy, temperature programmed desorption, and charge calculation results revealed that the active sites for the catalytic reaction were the carbon atoms bonded to the pyridinic N and positively charged nitrogen atoms (viologenic N^+) of the viologen moieties in cCTN-700, similar to the active sites in Au-based catalysts but different from the those in previously reported nitrogen-doped carbon materials. This research focuses on using cationic covalent triazine polymers for selective acetylene hydrochlorination.

Keywords: cationic covalent triazine network; metal-free catalysts; acetylene hydrochlorination; pyridinic N; viologenic N^+

1. Introduction

Poly(vinyl chloride) (PVC) is the third most widely produced synthetic polymer of plastic worldwide and has been processed to obtain various products owing to its excellent properties and low cost. The total global production volume of PVC amounted to 44.3 million metric tons in 2018, with a projected increase to ~60 million metric tons in 2025. Vinyl chloride monomer, the feedstock for PVC production, is synthesized mainly via acetylene hydrochlorination using $HgCl_2$ supported on activated carbon [1]. During hydrochlorination, however, the catalyst is environmentally toxic with relatively short lifetimes because the $HgCl_2$ is apt to sublime during reaction [2]. Therefore, nonmercury heterogeneous catalysts, including Au-based catalysts [3–9] and non-noble-metal-based catalysts [10–15], have been widely investigated for acetylene hydrochlorination. Although metal-based catalysts exhibit high catalytic activities, their high cost and poor durability considerably restrict their commercialization [10,16,17]. Recently, nitrogen-doped carbon materials have attracted the attention of many researchers owing to their good performance in acetylene hydrochlorination [18–23]. For example, a nanocomposite of nitrogen-doped silicon carbide material (SiC@N–C) reported by Bao and coworkers showed stable catalytic activity and high conversion during acetylene hydrochlorination (~80% at 200 °C with a space velocity of 0.8 mL g^{-1} min^{-1}), and the carbon atoms adjacent to pyrrolic nitrogen atoms were proposed to be the active sites in SiC@N-C [24]. Although other research groups have developed nitrogen-doped carbon catalysts for acetylene hydrochlorination using

pyridinic-N or quaternary-N active sites [2,18,21,22,25,26], challenges remain in designing and constructing nitrogen-doped carbon catalysts with a precise number of N active sites and prototypes for acetylene hydrochlorination. Triazine piqued our interest while we were searching for potential monomers to build nitrogen-doped carbon materials as catalysts for acetylene hydrochlorination. We envisioned that the basicity of triazine N in the carbon matrix could promote hydrogen–chloride absorption, while acetylene, as a nucleophile, is inclined to be attracted by the positively charged nitrogen atoms in viologen moieties. Therefore, we focused on developing cationic covalent triazine networks (cCTNs) using triazine and viologen as building blocks.

Herein, we report our cationic viologen-based covalent triazine networks fabricated as a metal-free nitrogen-doped carbon catalyst for selective acetylene hydrochlorination. cCTNs exhibited excellent catalytic activity, with initial acetylene conversion reaching ~99% and a vinyl chloride selectivity of >98% at 200 °C during a 45 h test. This catalytic result reached the mercury chloride catalyst, exceeding the reported nitrogen-doped carbon catalyst. cCTNs have a similar catalytic mechanism to mercury chloride. The positive charge on the surface of the catalyst is similar to that of mercury ion, which can enhance the adsorption of acetylene. Pyridine nitrogen is similar to chloride ion, which can adsorb hydrogen chloride molecules. The catalytic mechanism of the nitrogen-doped carbon catalysts is dependent mainly on pyridine nitrogen adsorption of hydrogen chloride molecules, while the adsorption capacity of acetylene molecules is weak.

2. Results

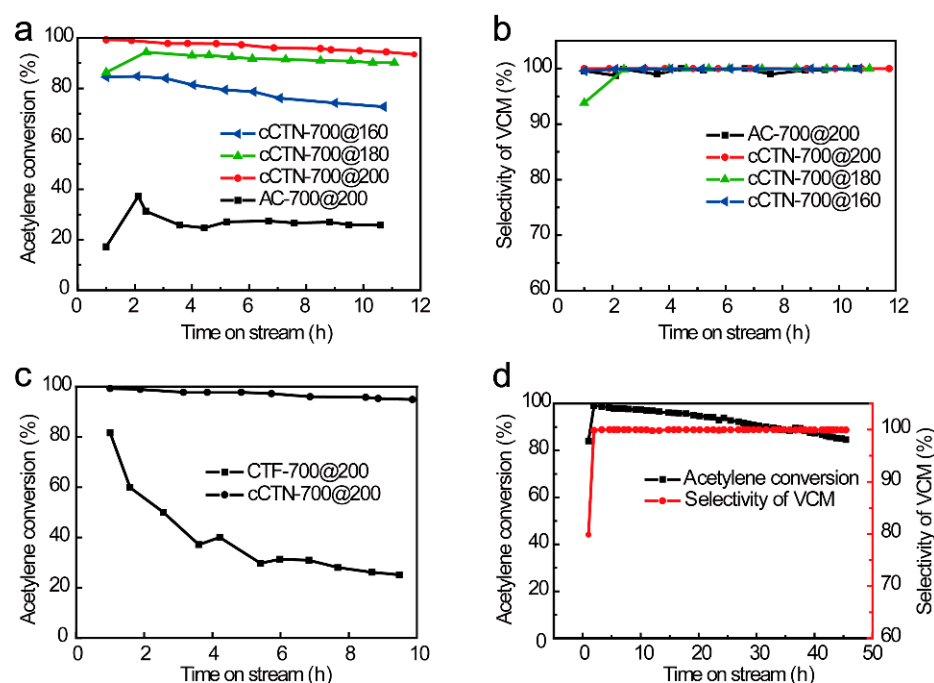### 2.1. Catalytic Performance of cCTN-700

In a fixed-bed reactor, acetylene hydrochlorination was conducted at various reaction temperatures using cCTN-700 as a catalyst to determine its catalytic performance. As shown in Figure 1, acetylene conversion considerably increased with increasing reaction temperature and the initial acetylene conversion at 200 °C surprisingly reached 99.3% with a vinyl chloride selectivity of 98% (Figure 1a,b), outperforming the previously reported N-doped catalysts [24,27,28]. By contrast, the CTF-700 catalyst exhibited a rather low activity, with an initial acetylene conversion of 81.6% (Figure 1c), which quickly dropped to 25.2% after a 10 h test. cCTN-700 demonstrated stable acetylene hydrochlorination during a 45 h test (Figure 1d), showing the superiority of cCTN-700 over CTF-700 in terms of catalytic stability. cCTN-700 showed a great potential for use as a metal-free catalyst to replace the mercury catalyst in the poly(vinyl chloride) industry.

2.2. Structure–Activity Relationship

The elemental analysis of CTF-700 and cCTN-700 indicated that CTF-700 exhibited a slightly higher nitrogen content than cCTN-700. Previous studies indicated that increasing the nitrogen content of N-doped carbon catalysts improved their catalytic performance in acetylene hydrochlorination [3,26]. Thus, the nitrogen content could not explain the catalytic performance of cCTN-700, which appeared to be attributed to the viologen units in its structure. The surface morphologies and textures of cCTN:Cl, CTF, cCTN-700, and CTF-700 were studied using SEM (Figure 2). The SEM images of cCTN-700 (Figure 2a,b) show that it retained the intrinsic morphology of cCTN:Cl, indicating that cCTN-700 was perfectly fabricated via pyrolysis of cCTN:Cl. However, the texture of the cCTN-700 appears much looser and more porous than those of cCTN:Cl and CTF-700, implying that the increased special surface in cCTN-700 benefitted its catalytic performance (Figure 2).

According to the IUPAC classification, the N_2 adsorption/desorption of cCTN-700 showed a type IV isotherm (Figure 2e,f). The total adsorption capacity at the relative pressure (0–1.0) was only ~28 cm^3 g^{-1}, indicating a small number of pores and low specific surface, consistent with the specific surface area data (17.0 m^2 g^{-1}) shown in Table 1. A type-H_3 hysteresis loop was obtained owing to capillary condensation at relative pressure P/P_0, widely ranging from 0.05 to 1.0, and no obvious saturated adsorption platform was observed, indicating abundant mesopores in the structure together with a small proportion

of micropores and macropores. Thus, the pore morphology of cCTN-700 was highly irregular. The isotherm also demonstrated that the pore-size distribution of the cCTN-700 was considerably wide, consistent with the pore-size distribution (PSD) plot (the inset presented in Figure 2e). The N_2 adsorption/desorption isotherm and PSD plot of the precursor cCTN:Cl showed a thermal deformation at 700 °C, resulting in an irregular morphology and space structure of cCTN-700. The low molecular weight of cCTN-700 was attributed to the depolymerization of cCTN:Cl at a high temperature (700 °C), consistent with SEM images (Figure 2a,b). By contrast, the precursor CTF seemed to exhibit a different thermal deformation, resulting in a small number of pores and low specific surface area of CTF-700 (Figure 2f and Table 1). The N_2 isotherms and PSD plots of CTF and CTF-700 were consistent with the SEM images presented in Figure 2c,d. cCTN-700 exhibited a higher specific surface area than the CTF-700, indicating its excellent catalytic performance in acetylene hydrochlorination. Nonetheless, the specific surface area of cCTN-700 was considerably lower than that of an activated carbon-based catalyst. Thus, it is speculated that the excellent superior catalytic performance of cCTN-700 could be attributed to its intrinsic highly active sites.


Figure 1. (**a**) Acetylene conversion under various reaction temperatures (160–200 °C). (**b**) Selectivity of vinyl chloride. (**c**) Comparison of the catalytic performance of cCTN-700 and CTF-700 at 200 °C. (**d**) Stability test of cCTN-700. Reaction conditions: T = 160–200 °C, 1 atm, feed mole ratio hydrogen chloride/C_2H_2 = 1.2, and C_2H_2 space velocity = 1.0 mL min^{-1} g^{-1} (gas hourly space velocity (GHSV) = 40 h^{-1}).

Table 1. Elemental compositions and texture properties of the catalysts.

| Sample	C% [a]	O% [a]	H% [a]	N% [a]	SBET [b] (m²/g)	D Average [c] (nm)	Nitrogen–Carbon Ratio
cCTN:Cl	59.6	11.4	4.7	14.2	/	/	0.24
CTF	65.5	9.5	4.1	18.7	/	/	0.29
cCTN-700	79.4	3.8	1.8	11.3	17.0	5–10	0.21
CTF-700	82.3	2.9	1.6	12.3	5.7	30–40	0.07

[a] Measured via combustion elemental analysis; [b] specific surface area; [c] adsorption average pore width.
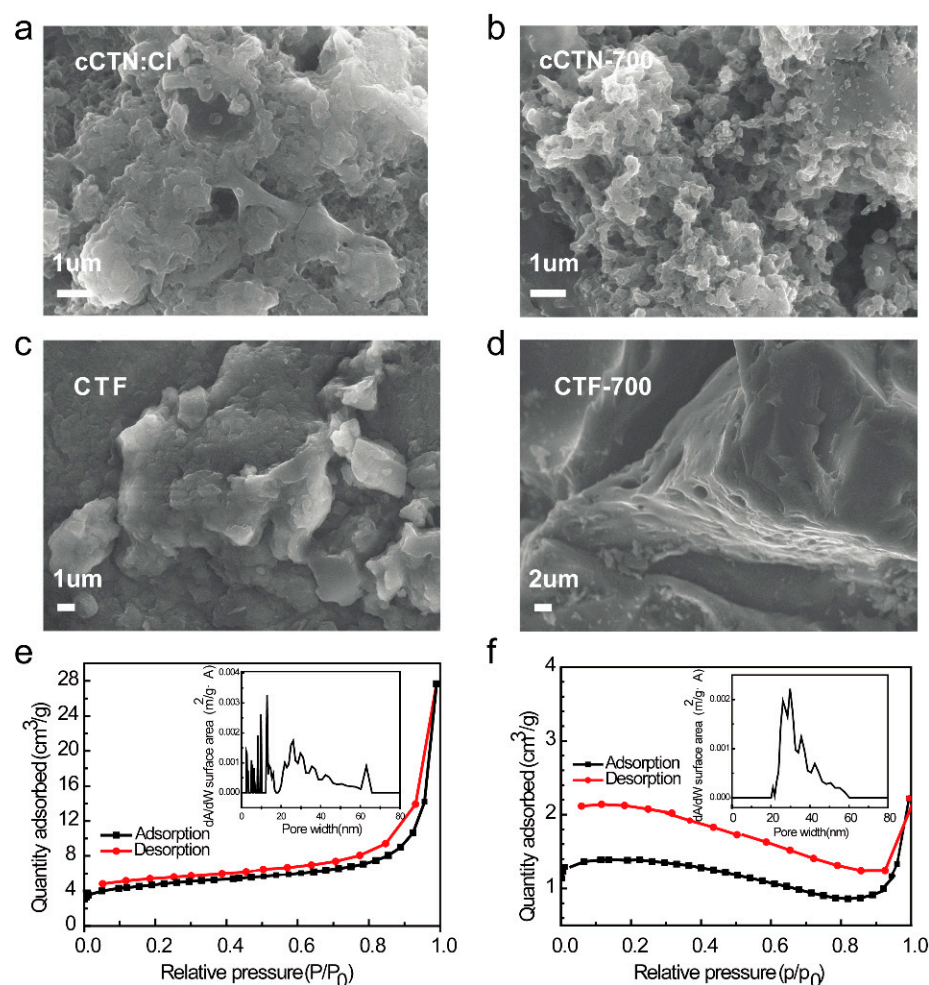
Figure 2. (**a–d**) SEM images of (**a**) cCTN:Cl, (**b**) cCTN-700, (**c**) CTF, and (**d**) CTF-700. (**e,f**) N_2 adsorption–desorption isotherms of (**e**) cCTN-700 and (**f**) CTF-700; insets: the corresponding PSD of (**e**) cCTN-700 and (**f**) CTF-700.

In the Raman spectra of cCTN-700 and CTF-700 (Figure 3a), the appearance of diffraction peaks at 1595 cm^{-1} (the G band) and 1352 cm^{-1} (the D band) could be attributed to the ordered carbon structure associated with the sp^2 electronic configuration and the disordered/defective structure of carbon, respectively. The intensity ratio of the D/G peaks (I_D/I_G) was generally correlated with the defective degree of carbon materials. The doping of nitrogen atoms led to the generation of defects and the difference of their catalytic activity. cCTN-700 and CTF-700 showed approximately equivalent I_D/I_G values (Figure 3a), indicating that these materials exhibited the close defective degree. Their XRD patterns were obtained to further detect crystals and defects on the surface of the materials (Figure 3b). The strong peaks located at ~24.5° and ~43.5° could be assigned to the (002) and (100) crystal planes of graphite structure, respectively. The position (angle) of the (002) band was believed to be related to the interlayer spacing between aromatic layers. The intensities of the (002) crystal planes of cCTN-700 and CTF-700 were high, implying the formation of ordered graphitized structures. The higher intensities of the (002) and (100) bands of CTF-700, compared with those of cCTN-700, implied a higher graphitization degree of the former than that of the latter. Such a difference in the graphitization degree of the two materials could also be attributed to the viologen units present in cCTN-700. It is assumed that the superior catalytic performance of cCTN-700 was attributed to the viologen units in the carbon skeleton.
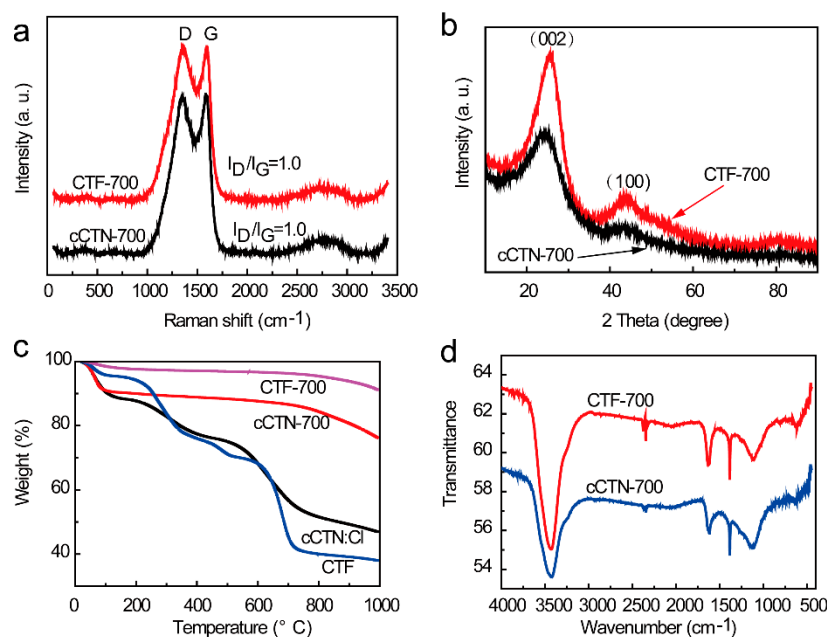
Figure 3. (**a**) Raman spectra of cCTN-700 and CTF-700. (**b**) PXRD patterns of cCTN-700 and CTF-700. (**c**) TGA patterns of the samples were recorded under nitrogen atmosphere. (**d**) FTIR spectra of cCTN-700 and CTF-700.

The TGA of cCTN:Cl and CTF conducted under nitrogen atmosphere showed substantial weight loss from 100 °C to 700 °C (Figure 3c), indicating the poor thermal stability of the two materials in this temperature range, but high thermal stabilities were observed between 700 °C and 1000 °C (no obvious weight loss). Furthermore, on the basis of the TGA curves, the precursor cCTN:Cl appeared to exhibit a higher thermal stability than CTF. Therefore, calcination of both precursors, cCTN:Cl and CTF, was performed at 700 °C to afford cCTN-700 and CTF-700, respectively, with high thermal stability.

The catalysts cCTN-700 and CTF-700 showed very similar patterns in their Fourier-transform infrared (FTIR) spectra (Figure 3d), with the characteristic C=N, C–N and benzene C–H stretching bands observed at 1550, 1360, and 3300 cm^{-1}, respectively, implying the presence of triazine and benzene moieties.

2.3. Active Sites and Mechanism of Catalytic Acetylene Hydrochlorination

XPS, TPD, and the calculations of total charges of molecules were performed to gain an insight into the active sites of cCTN-700 for acetylene hydrochlorination and the relation between the forms of nitrogen species and catalytic activity. In the XPS spectra (Figure 4a), the peaks observed at ~284, ~400, and ~530 eV could be assigned to C1s, N1s, and O1s, respectively. The peak observed at ~200 eV in the XPS spectrum of cCTN:Cl was assigned to Cl2p. The disappearance of the Cl2p signal in the XPS spectrum of cCTN-700 indicated disappearance of the positive charges after calcination of cCTN:Cl at 700 °C. To understand the chemical state of the nitrogen species, the high-resolution N1s spectra of CTF-700 and cCTN-700 were collected (Figure 4b,c). As shown in Figure 4b, the deconvolution of the high-resolution N1s spectrum of CTF-700 showed two peaks, corresponding to two chemical states attributed to pyridinic N (~398.5 eV) and graphitic N (~401.2 eV). At an elevated calcination temperature, the triazine nitrogen atoms of CTF, which were often categorized as pyridinic N in catalyst chemistry, were partially converted into graphitic N. By contrast, the high-resolution N1s spectrum of cCTN-700 was split into three peaks, corresponding to pyridinic N (~398.5 eV), graphitic N (~401.2 eV), and viologenic N (~402 eV), as pyridinic N and viologenic N could partially convert to graphitic N. On the basis of the difference in the composition of the chemical state of N in these two catalysts,

we propose that the viologen nitrogen species in cCTN-700 caused its excellent catalytic activity in acetylene hydrochlorination, with initial acetylene conversion of >98%.
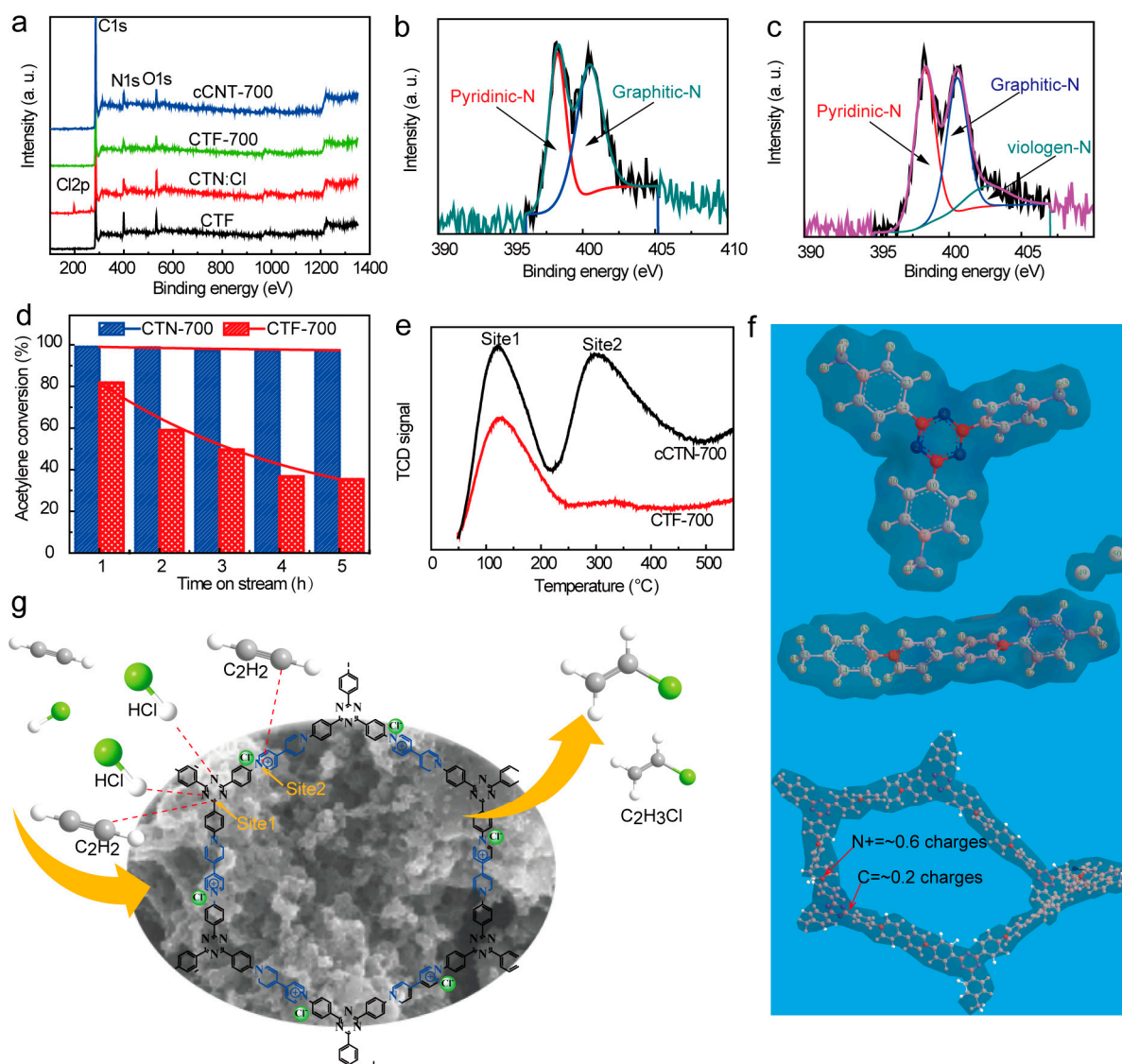
Figure 4. (**a**) XPS spectra of CTF, CTN:Cl, CTF-700, and cCTN-700. (**b**) High-resolution N1s spectrum of CTF-700. (**c**) High-resolution N1s spectrum of cCTN-700. (**d**) Catalytic performance of CTF-700 and cCTN-700 for acetylene hydrochlorination; reaction conditions: T = 200 °C, atmospheric pressure, feed mole ratio hydrogen chloride/C_2H_2 = 1.2, and C_2H_2 space velocity = 1.0 mL min^{-1} g^{-1} (GHSV = 40 h^{-1}). (**e**) TPD of acetylene on CTF-700 and cCTN-700. (**f**) Charge models of triazine unit, 4,4′-bipyridine unit, and cCTN-700. Color code: red for positive charges and blue for negative charges. (**g**) Mechanistic illustration of acetylene hydrochlorination.

TPD enables the determination of the binding strength of the adsorbed species on the catalyst surface and the amounts of species adsorbed. As shown in Figure 4e, two acetylene-desorption temperature peaks were observed for cCTN-700 at ~130 °C and ~300 °C, but only one acetylene-desorption peak was observed for CTF-700 at ~130 °C. The desorption peak observed at ~130 °C was assigned to the pyridinic N in CTF-700 or cCTN-700, and the acetylene-desorption peak observed at ~300 °C for cCTN-700 was, thus, assigned to the species of viologenic N.

The pyridinic N and carbons bonded to the pyridinic N in CTF-700 were the active sites for adsorbing hydrogen chloride and acetylene, respectively [1,24]. The carbon site (Site 1) in cCTN-700 showed the same adsorbing and activating ability for acetylene as that

in CTF-700; however, the N^+ site of the viologen moieties (Site 2) in cCTN-700 exhibited higher adsorbing and activating ability. These results were consistent with the activity data (Figure 4d). The result of TPD further demonstrated that the N^+ sites of the viologen moieties in cCTN-700 played a critical role in acetylene hydrochlorination in addition to the carbons bonded to the pyridinic N.

The charge distributions of triazine, 4,4′-bipyridine, and the $cCTN^+$ moiety were calculated to better understand the active sites of cCTN-700 for acetylene hydrochlorination (Figure 4f). Positive charges of ~0.6 and ~0.2 were found on the atomic orbitals of viologenic N^+ and a carbon atom bonded with pyridinic N, respectively. Owing to the difference in positive charges, the adsorbing and activating ability of viologenic N^+ for acetylene was superior to that of a carbon atom bonded with pyridinic N, consistent with the results presented in Figure 4d,e. The mechanism of acetylene hydrochlorination catalyzed by cCTN-700 is shown in Figure 4g. According to the TPD results [21,23], adsorbing hydrogen chloride is the rate-limiting step in this catalytic acetylene hydrochlorination because the adsorption ability of pyridinic N for hydrogen chloride is similar to that of a carbon atom bonded with pyridinic N for acetylene. Excess hydrogen chloride was fed and adsorbed onto pyridinic N, whereas acetylene was fed and adsorbed onto carbon atoms bonded with pyridinic N and viologenic N^+ of cCTN-700. After being activated, hydrogen chloride reacted with acetylene to form vinyl chloride, which was then released from the cCTN-700 surface.

3. Materials and Methods

3.1. Catalyst Precursor Synthesis

3.1.1. Synthesis of Precursor Catalyst cCTN:Cl

According to our previous report, the precursor of the cCTN was prepared via Zincke reaction [28,29]. 2,4,6-Tris(4-aminophenyl)-1,3,5-triazine (TAPT) (354.0 mg, 1.0 mmol) and 1,1′-bis(4-cyanophenyl)-[4,4′-bipyridine]-1,1′-diium dichloride (DNP^{2+}-$2Cl^-$) (841.5 mg, 1.5 mmol) were dispersed in a mixed solvent containing EtOH and H_2O (50 mL, 10:1, v v^{-1}) within a sealed tube. The resulting mixture was sonicated for 30 min and then heated at 120 °C for 72 h. Subsequently, the reaction mixture was cooled to 25 °C, and the resulting precipitate was collected via filtration; washed with THF, water, and EtOH; and dried at 120 °C under reduced pressure to obtain the cationic viologen-based covalent triazine networks cCTN:Cl (0.71 g, 59%) (Scheme 1).
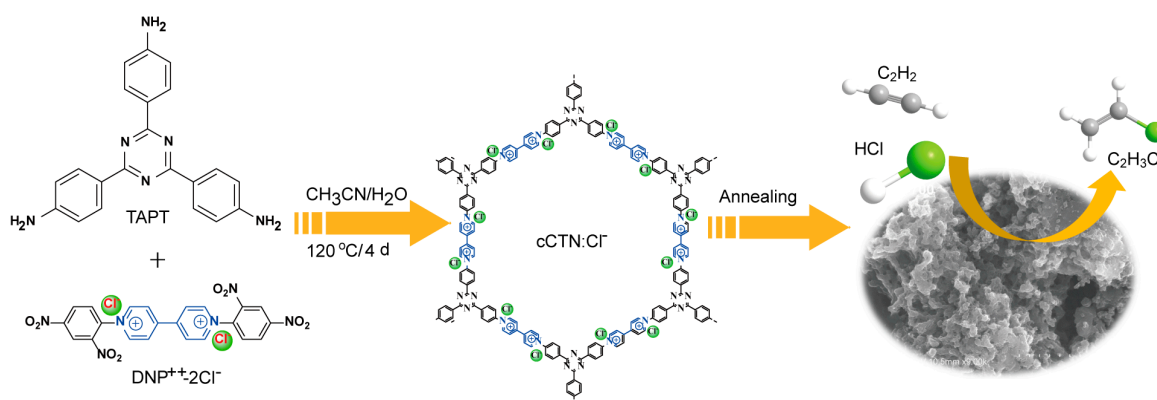
Scheme 1. Preparation of cationic viologen-based covalent triazine networks (cCTN:Cl).

3.1.2. Synthesis of Precursor Covalent Triazine Networks (CTN) [30,31]

Trifluoromethanesulfonic acid (20 mL) was dropwise added to a round bottom flask containing terephthalonitrile (2.56 g, 20 mmol) at room temperature under Ar atmosphere, affording a red solution that was heated overnight at 100 °C. After being cooled to room temperature, the reaction mixture was poured onto ice, and the resulting mixture was neutralized to pH = 7 using a concentrated aqueous ammonia solution (28%). The formed

yellow precipitate was collected via filtration, washed with water, and dried under reduced pressure at 80 °C for 12 h to obtain CTN as a reddish-brown power.

3.1.3. Preparation of Catalyst cCTN-700

The as-synthesized cCTN:Cl (5.0 g) was carbonized at 700 °C for 2 h under nitrogen atmosphere at a heating rate of 5 °C min^{-1}. After being cooled to room temperature, the obtained black powder was washed with an aqueous hydrogen chloride solution (2.0 M) and water (pH = 7) and dried under reduced pressure at 80 °C for 12 h to obtain catalyst cCTN-700 (2.5 g, 50%).

3.1.4. Preparation of Catalyst CTF-700

The covalent triazine framework CTF-700 was prepared using CTF by following a similar procedure as that of the preparation of cCTN-700.

3.2. Catalyst Characterization

The stabilities of the as-synthesized catalysts were analyzed using thermogravimetric analysis (TGA) on a SDT Q600 thermogravimetric analyzer (TA Instruments, New Castle, DE, USA) at a heating rate of 10 °C min^{-1} from room temperature to 1000 °C under nitrogen atmosphere. The crystalline structures of the catalysts were determined using power X-ray diffraction (PXRD) on a Bruker AXS D8 ADVANCE X-ray diffractometer with Cu Kα radiation (Bruker D8, Bruker AXS, Bruker Company, Karlsruhe, Germany). The microstructures of samples were obtained via scanning electron microscopy (SEM) using a Hitachi S-4800 field-emission scanning electron microscope (S-4800, Hitachi Company, Tokyo, Japan). X-ray photoelectron spectroscopy (XPS) was conducted using a Thermo Scientific Kα X-ray photoelectron spectrometer fitted with a monochromatic Al Kα source (EscaLab 250Xi, Thermo Fisher Scientific Company, Waltham, MA, USA). Elemental analysis (EA) was performed using a Perkin Elmer PE2400CHNS instrument (Perkin Elmer Company, Waltham, MA, USA). The N$_2$ adsorption/desorption isotherms were measured using a JW-BK122W surface area and pore-size distribution analyzer at 77 K (JWGB Company, Beijing, China). The Raman spectra were recorded using a Raman spectrometer with a 532 nm laser excitation (iuVia reflex, Ren-ishaw Company, London, UK). Temperature programmed desorption (TPD) study of acetylene was performed using a Micromeritic ASAP 2720 instrument with a temperature ramp of 50–600 °C at a ramp rate of 10 °C min^{-1} and a He flow of 45 mL min^{-1} (ASAP 2720, Micromeritics Company, Norcross, GA, USA).

3.3. Catalytic Performance

The catalytic performance regarding acetylene hydrochlorination was evaluated using a fixed-bed quartz tube microreactor. After loading the catalyst into the tube, air and water were removed by flowing high-purity N$_2$ (10 mL min^{-1}) at 150 °C. After activating the catalysts using hydrogen chloride (10 mL min^{-1}) for 1 h, acetylene (1.0 mL min^{-1}) and hydrogen chloride (1.2 mL min^{-1}) were introduced into the reactor, and the reaction was monitored every one hour.

4. Conclusions

We developed a new type of nanocomposite cCTN-700 that can selectively catalyze acetylene hydrochlorination to afford vinyl chloride. cCTN-700 exhibited an excellent catalytic activity, with acetylene conversion reaching ~99% and selectivity to vinyl chloride as >98% at a space velocity of 1.0 mL min^{-1} g^{-1} at 200 °C. Furthermore, the catalyst demonstrated good stability in a 45 h test. XPS analysis and catalytic activity data revealed that the carbon atoms bonded to the pyridinic N and viologenic N$^+$ at the sites that adsorb and activate acetylene; these sites are obviously different from those in the other reported nitrogen-doped carbon materials [2,16–19,23]. The present study demonstrates that cCTN-700 can be used as a catalyst to substitute the toxic HgCl$_2$ catalyst for acetylene hydrochlorination.

References

1. Sun, S.; Xu, H.; Fan, Y.; Liu, Z.; Hong, Q.; Huang, W.; Qu, Z.; Yan, N. Construction of a Thermally Stable Low-HgCl$_2$ Catalyst via Chalcogen Bonding and Its Enhanced Activity in Acetylene Hydrochlorination. *Ind. Eng. Chem. Res.* **2022**, *61*, 17057–17064. [CrossRef]

2. Chao, S.; Zou, F.; Wan, F.; Dong, X.; Wang, Y.; Wang, Y.; Guan, Q.; Wang, G.; Li, W. Nitrogen-doped Carbon Derived from ZIF-8 as a High-performance Metal-free Catalyst for Acetylene Hydrochlorination. *Sci. Rep.* **2017**, *7*, 39789. [CrossRef]

3. Zhang, H.; Dai, B.; Wang, X.; Xu, L.; Zhu, M. Hydrochlorination of Acetylene to Vinyl Chloride Monomer over Bimetallic Au–La/SAC Catalysts. *J. Ind. Eng. Chem.* **2012**, *18*, 49–54. [CrossRef]

4. Hutchings, G.J.; Haruta, M. A Golden Age of Catalysis: A Perspective. *Appl. Catal. A* **2005**, *291*, 2–5. [CrossRef]

5. Li, G.B.; Li, W.; Zhang, J.L. Non-mercury Catalytic Acetylene Hydrochlorination over Activated Carbon-Supported Au Catalysts Promoted by CeO$_2$. *Catal. Sci. Technol.* **2016**, *6*, 1821–1828. [CrossRef]

6. Huang, C.; Zhu, M.; Kang, L.; Li, X.; Dai, B. Active Carbon Supported TiO$_2$-AuCl$_3$/AC Catalyst with Excellent Stability for Acetylene Hydrochlorination Reaction. *Chem. Eng. J.* **2014**, *242*, 69–75. [CrossRef]

7. Huang, C.F.; Zhu, M.Y.; Kang, L.H.; Dai, B. A Novel High-Stability Au(III)/Schiff-Based Catalyst for Acetylene Hydrochlorination Reaction. *Cat. Commun.* **2014**, *54*, 61–65. [CrossRef]

8. Zhao, J.; Gu, S.C.; Xu, X.L.; Zhang, T.T.; Yu, Y.; Di, X.X.; Ni, J.; Pan, Z.Y.; Li, X.N. Supported Ionic-Liquid-Phase-Stabilized Au(III) Catalyst for Acetylene Hydrochlorination. *Catal. Sci. Technol.* **2016**, *6*, 3263–3270. [CrossRef]

9. Hu, J.Y.; Yang, Q.W.; Yang, L.F.; Zhang, Z.G.; Su, B.G.; Bao, Z.B.; Ren, Q.L.; Xing, H.B.; Dai, S. Confining Noble Metal (Pd, Au, Pt) Nanoparticles in Surfactant Ionic Liquids: Active Non-mercury Catalysts for Hydrochlorination of Acetylene. *ACS Catal.* **2015**, *5*, 6724–6731. [CrossRef]

10. Zhang, H.; Dai, B.; Wang, X.; Li, W.; Han, Y.; Gu, J.; Zhang, J. Non-mercury Catalytic Acetylene Hydrochlorination over Bimetallic Au-Co (III)/SAC Catalysts for Vinyl Chloride Monomer Production. *Green Chem.* **2013**, *15*, 829–836. [CrossRef]

11. Zhang, H.Y.; Li, W.; Li, X.Q.; Zhao, W.; Gu, J.J.; Qi, X.Y.; Dong, Y.Z.; Dai, B.; Zhang, J.L. Non-mercury Catalytic Acetylene Hydrochlorination over Bimetallic Au-Ba (II)/AC Catalysts. *Catal. Sci. Technol.* **2015**, *5*, 1870–1877. [CrossRef]

12. Zhang, H.Y.; Li, W.; Jin, Y.H.; Sheng, W.; Hu, M.C.; Wang, X.Q.; Zhang, J.L. Ru-Co (III)-Cu(II)/SAC Catalyst for Acetylene Hydrochlorination. *Appl. Catal. B-Environ.* **2016**, *189*, 56–64. [CrossRef]

13. Zhao, W.L.; Zhu, M.Y.; Dai, B. The Preparation of Cu-g-C$_3$N$_4$/AC Catalyst for Acetylene Hydrochlorination. *Catalysts.* **2016**, *6*, 193. [CrossRef]

14. Hu, D.; Wang, F.; Wang, J. Bi/AC Modified with Phosphoric Acid as Catalyst in the Hydrochlorination of Acetylene. *RSC Adv.* **2017**, *7*, 7567–7575. [CrossRef]

15. Qi, H.; Li, Q.; Mo, Z.S.; Zhang, X.T.; Song, L.J. MCl$_2$ (M = Hg, Cd, Zn, Mn) Catalysed Hydrochlorination of Acetylene—A Density Functional Theory Study. *Mol. Simul.* **2017**, *43*, 28–33. [CrossRef]

16. Zhu, M.; Wang, Q.; Chen, K.; Wang, Y.; Huang, C.; Dai, H.; Yu, F.; Kang, L.; Dai, B. Development of a Heterogeneous Non-Mercury Catalyst for Acetylene Hydrochlorination. *ACS Catal.* **2015**, *5*, 5306–5316. [CrossRef]

17. Yang, Y.; Lan, G.J.; Wang, X.L.; Li, Y. Direct Synthesis of Nitrogen-Doped Mesoporous Carbons for Acetylene Hydrochlorination. *Chin. J. Catal.* **2016**, *37*, 1242–1248. [CrossRef]

18. Zhang, T.T.; Zhao, J.; Xu, J.T.; Xu, J.H.; Di, X.X.; Li, X.N. Oxygen and Nitrogen-Doped Metal-Free Carbon Catalysts for Hydrochlorination of Acetylene. *Chin. J. Chem. Eng.* **2016**, *24*, 484–490. [CrossRef]

19. Li, X.Y.; Pan, X.L.; Bao, X.H. Nitrogen Doped Carbon Catalyzing Acetylene Conversion to Vinyl Chloride. *J. Energy Chem.* **2014**, *23*, 131–135. [CrossRef]

20. Zhao, F.; Wang, Y.; Zhu, M.Y.; Kang, L.H. C-Doped Boron Nitride Fullerene as a Novel Catalyst for Acetylene Hydrochlorination: A DFT Study. *RSC Adv.* **2015**, *5*, 56348–56355. [CrossRef]

21. Zhang, C.L.; Kang, L.H.; Zhu, M.Y.; Dai, B. Nitrogen-Doped Active Carbon as a Metal-Free Catalyst for Acetylene Hydrochlorination. *RSC Adv.* **2015**, *5*, 7461–7468. [CrossRef]

22. Dai, B.; Chen, K.; Wang, Y.; Kang, L.H.; Zhu, M.Y. Boron and Nitrogen Doping in Graphene for the Catalysis of Acetylene Hydrochlorination. *ACS Catal.* **2015**, *5*, 2541–2547. [CrossRef]

23. Wang, X.; Dai, B.; Wang, Y.; Yu, F. Nitrogen-Doped Pitch-Based Spherical Active Carbon as a Nonmetal Catalyst for Acetylene Hydrochlorination. *ChemCatChem* **2014**, *6*, 2339–2344. [CrossRef]

24. Li, X.; Pan, X.; Yu, L.; Ren, P.; Wu, X.; Sun, L.; Jiao, F.; Bao, X. Silicon Carbide-Derived Carbon Nanocomposite as a Substitute for Mercury in the Catalytic Hydrochlorination of Acetylene. *Nat. Commun.* **2014**, *5*, 3688. [CrossRef]

25. Zhou, K.; Li, B.; Zhang, Q.; Huang, J.Q.; Tian, G.L.; Jia, J.C.; Zhao, M.Q.; Luo, G.H.; Su, D.S.; Wei, F. The Catalytic Pathways of Hydrohalogenation over Metal-Free Nitrogen-Doped Carbon Nanotubes. *ChemSusChem* **2014**, *7*, 723–728. [CrossRef]

26. Li, X.; Wang, Y.; Kang, L.; Zhu, M.; Dai, B. A Novel, Non-metallic Graphitic Carbon Nitride Catalyst for Acetylene Hydrochlorination. *J. Catal.* **2014**, *311*, 288–294. [CrossRef]

27. Zhou, X.; Wang, P.L.; Zhang, Y.G.; Wang, L.L.; Zhang, L.T.; Zhang, L.; Xu, L.; Liu, L. Biomass Based Nitrogen-Doped Structure-Tunable Versatile Porous Carbon Materials. *J. Mater. Chem. A* **2017**, *5*, 12958–12968. [CrossRef]

28. Buyukcakir, O.; Je, S.H.; Talapaneni, S.N.; Kim, D.; Coskun, A. Charged Covalent Triazine Frameworks for CO_2 Capture and Conversion. *ACS Appl. Mater. Interfaces* **2017**, *9*, 7209–7216. [CrossRef]

29. Peng, L.Z.; Liu, P.; Cheng, Q.Q.; Hu, W.J.; Liu, Y.A.; Li, J.S.; Jiang, B.; Jia, X.S.; Yang, H.; Wen, K. Highly Effective Electrosynthesis of Hydrogen Peroxide from Oxygen on a Redox-Active Cationic Covalent Triazine Network. *Chem. Commun.* **2018**, *54*, 4433–4436. [CrossRef]

30. Niyogi, S.; Bekyarova, E.; Itkis, M.E.; Zhang, H.; Shepperd, K.; Hicks, J.; Sprinkle, M.; Berger, C.; Lau, C.N.; de Heer, W.A.; et al. Spectroscopy of Covalently Functionalized Graphene. *Nano Lett.* **2010**, *10*, 4061–4066. [CrossRef]

31. Li, X.; Li, P.; Pan, X.; Ma, H.; Bao, X. Deactivation Mechanism and Regeneration of Carbon Nanocomposite Catalyst for Acetylene Hydrochlorination. *Appl. Catal. B Environ.* **2017**, *210*, 116–120. [CrossRef]